



This is a repository copy of *Performance analysis of a hybrid ferrite IPM/SynR traction machine with axially combined rotor structure*.

White Rose Research Online URL for this paper:

<https://eprints.whiterose.ac.uk/190458/>

Version: Accepted Version

Proceedings Paper:

Hoang, K.D. orcid.org/0000-0001-7463-9681, Yu, A., Atallah, K. et al. (2 more authors) (2022) Performance analysis of a hybrid ferrite IPM/SynR traction machine with axially combined rotor structure. In: 11th International Conference on Power Electronics, Machines and Drives (PEMD 2022). 11th International Conference on Power Electronics, Machines and Drives (PEMD 2022), 21-23 Jun 2022, Hybrid Conference, Newcastle, UK. Institution of Engineering and Technology (IET) . ISBN 9781839537189

<https://doi.org/10.1049/icp.2022.1148>

© 2022 The Institution of Engineering and Technology. This is an author-produced version of a paper subsequently published in PEMD 2022 proceedings. Uploaded in accordance with the publisher's self-archiving policy.

Reuse

Items deposited in White Rose Research Online are protected by copyright, with all rights reserved unless indicated otherwise. They may be downloaded and/or printed for private study, or other acts as permitted by national copyright laws. The publisher or other rights holders may allow further reproduction and re-use of the full text version. This is indicated by the licence information on the White Rose Research Online record for the item.

Takedown

If you consider content in White Rose Research Online to be in breach of UK law, please notify us by emailing eprints@whiterose.ac.uk including the URL of the record and the reason for the withdrawal request.



eprints@whiterose.ac.uk
<https://eprints.whiterose.ac.uk/>

Performance Analysis of a Hybrid Ferrite IPM/SynR Traction Machine with Axially Combined Rotor Structure

Khoa Dang Hoang¹, Anshan Yu², Kais Atallah², Giorgio Valente³, Annabel Shahaj³

¹*Department of Engineering and Technology, University of Huddersfield, HD1 3DH, Huddersfield, UK*

²*Department of Electronic and Electrical Engineering, University of Sheffield, S1 3JD, Sheffield, UK*

³*Romax Technology-part of Hexagon, Ergo House, NG11 6JS, Nottingham, UK
d.k.hoang@hud.ac.uk*

Keywords: Ferrite IPM machine, hybrid rotor, synchronous reluctance (SynR) machine, WLTP driving cycle.

Abstract

The paper presents the performance analysis of a hybrid Ferrite Interior Permanent Magnet (IPM)/synchronous reluctance (SynR) traction machine with axially combined rotor structure. First, a hybrid rotor with axially combined structure of Ferrite IPM rotor and SynR rotor is introduced. Then, performance analysis is presented. It is shown that due to the axially combined structure, the hybrid concept machine could achieve a significant lower copper and iron loss in the high-speed operation region, compared with the original Ferrite IPM machine. It is demonstrated that due to the difference in optimum operation between the IPM and SynR machines, the two-rotor parts could be circumferentially shifted by an optimum angle for a specific control target achievement, i.e., maximum torque per ampere (MTPA) or minimum energy consumption over a specific driving cycle. Therefore, an extra degree of freedom on design could be obtained for the hybrid rotor structure. The proposed concept is validated via FEA benchmarking by a high-speed high-power (12,000rpm and 80kW) Ferrite IPM traction machine. It is shown that in comparison with the Ferrite IPM machine, a reduction up to 26.29% in energy consumption over WLTP driving cycle could be achieved for the proposed hybrid rotor concept machine.

1 Introduction

Due to high-efficiency and high-speed operation achievement, interior permanent magnet (IPM) machine is often employed for traction applications of which performances are validated via a specific driving cycle [1], [2]. However, because of the high-cost as well supply-chain uncertainties of rare-earth PM, non-rare-earth PM traction machine technology is attracting significant interests from both academy and industry. In [3] and [4], a Ferrite IPM traction machine concept employing axial magnet to enhance the airgap flux density was respectively proposed and demonstrated via prototype measurement. However, in the high-speed operation region with field-weakening (FW) control, PM machines are subject to high copper losses due to high d -axis current required for maintaining a constant voltage magnitude under a specific DC-link voltage [1]. In [2], it was shown that a high injected d -axis current in IPM traction machine may result in high spatial harmonics leading to significant iron-loss.

On the other hand, synchronous reluctance (SynR) machine with non-PM employment, simple and robust rotor structure, as well as low-cost manufacture is also an attractive candidate for development of non-rare-earth PM traction machine concept [5]. In addition, due to its non-PM employment, a lower copper loss and iron-loss in the high-speed operation region could be achieved for SynR machine. However, since only reluctance torque is utilized, SynR machines are subject to low efficiency as well as low torque density, especially in the high-speed operation region, compared with PM machines [5]. Therefore, a hybrid rotor with axially combined rotor structure to exploit both advantages of PM machine and SynR

machine is often employed [6]-[9] and this is the target of the paper.

In [6] and [7], a two-part rotor concept including a surface-mounted PM (SPM) rotor part and SynR rotor part was presented. It was demonstrated that due to the saliency characteristics of the SynR rotor part, better FW operation could be achieved. More recently, similar rotor structure has been employed in [8] and [9] where it was shown that a hybrid rotor could provide better performance than the conventional PM-SynR machine with similar machine specifications and operation conditions.

In the paper, a hybrid rotor concept with axially combined structure of Ferrite IPM rotor and SynR rotor is presented and validate via FEA benchmarking by a high-speed high-power (12,000rpm and 80kW) Ferrite IPM traction machine. It is shown that the hybrid concept machine could achieve a significant lower copper and iron loss in the high-speed operation region, compared with the original Ferrite IPM machine. It is demonstrated that the circumferentially offset angle between the two-rotor parts could be adjusted for an optimum control target achievement (i.e., maximum torque per ampere or minimum energy consumption over a specific driving cycle). In comparison with the benchmark Ferrite IPM machine, a reduction up to 26.29% in energy consumption over the worldwide harmonised light vehicle test procedure (WLTP) driving cycle could be achieved for the proposed hybrid concept machine.

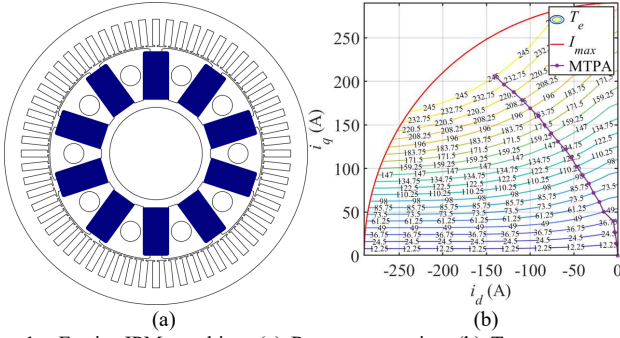


Fig. 1. Ferrite IPM machine. (a) Rotor geometries. (b) Torque map as a function of dq -axis currents.

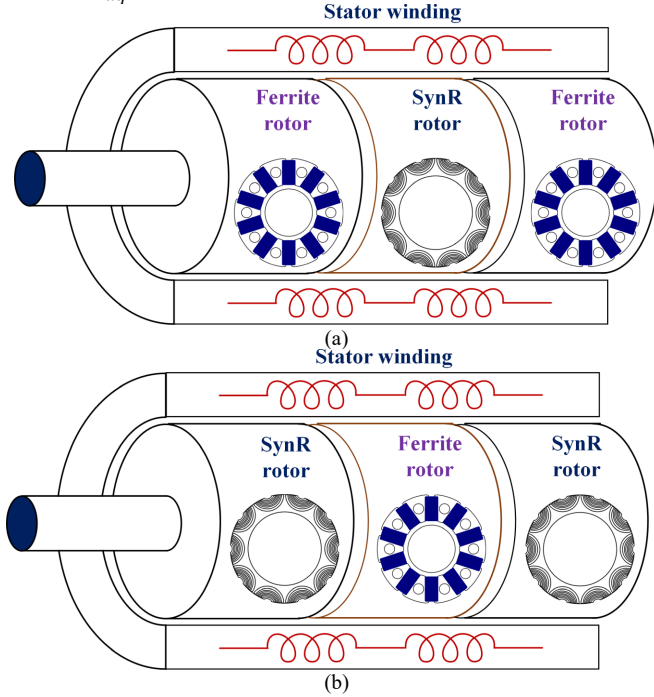


Fig. 2. Hybrid Ferrite IPM/SynR machine concept. (a) Combination of 2 Ferrite rotor stacks and 1 SynR rotor stack. (b) Combination of 1 Ferrite rotor stack and 2 SynR rotor stacks.

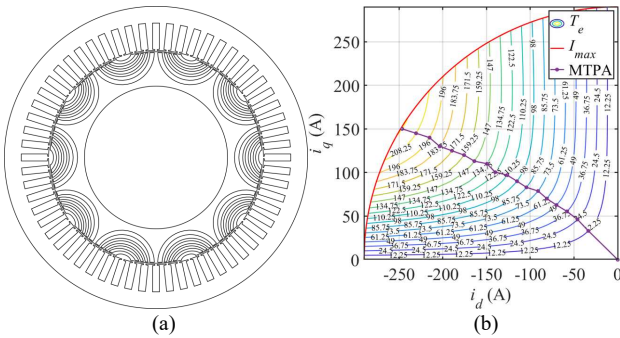


Fig. 3. SynR machine. (a) Rotor geometries. (b) Torque map as a function of dq -axis current.

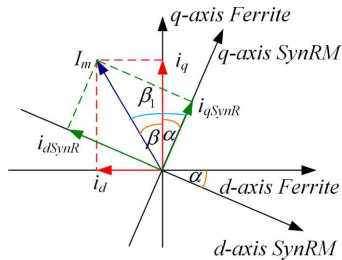


Fig. 4. Circumferentially shifted angle between Ferrite rotor stack and SynR rotor stack.

2 Hybrid rotor concept

Based on the Ferrite IPM machine concept with axial magnet in [2] and [3], a Ferrite IPM traction machine has been developed and validated. The machine specifications are described in Fig. 1, Table 1, and the machine loss maps (copper and iron loss) over torque-speed performance are presented in Fig. 7. As can be seen in Fig. 1(a), the designed machine has 10 poles and 60 stator slots. It is noted that to maximize the axial PM contribution, the ratio of axial length to rotor diameter of the Ferrite IPM machine should be minimized [2], [3]. Therefore, a multi-stack Ferrite IPM rotor is adopted. By replacing selected Ferrite IPM stacks of the Ferrite IPM machine by SynR stacks, two hybrid rotor concepts could be defined in Fig. 2. The geometry and torque map of the SynR machine with similar stator geometries and rotor active length as that of the Ferrite machine is presented in Fig. 3. It is noted that the target of the paper is the performance analysis of the hybrid rotor concept machine and therefore, optimum design details of both the Ferrite machine and the SynR machine is out of the scope of the paper.

Table 1 Ferrite machine design specifications

Peak/continuous torque (Nm)	120/245
Base/maximum speed (rpm)	3750/12000
Peak current (A)	290
DC-link voltage (V)	600

In comparison between Fig. 2(a) and Fig. 2(b), it is obvious that the concept in Fig. 2(a) with 2 Ferrite rotor stacks and 1 SynR rotor stack could have a higher torque capability in the low-speed operation region than the concept in Fig. 2(b) with 2 SynR rotor stacks and 1 Ferrite rotor stack [see Fig. 1(b) and 3(b)]. However, the concept in Fig. 2(b) may have a higher efficiency in the high-speed operation region. In the paper, due to space limitation, only analysis of the hybrid concept in Fig. 2(a) is introduced. It is noted that for each Ferrite rotor stack, its total length including the axial PM is higher than its active length without the axial PM (85mm vs 65mm) [4]. Thus, in the hybrid concept, a SynR rotor stack with active length as 85mm is employed to fit into the available space envelope.

The MTPA operation of the Ferrite IPM machine and the SynR machine is depicted in Figs. 1(b) and 3(b), respectively. As can be seen, for a given demanded torque, different dq -axis currents are required for each machine types. Therefore, for a hybrid rotor forming via axially combining of the Ferrite IPM rotor stacks and the SynR rotor stack, the two-rotor parts should be circumferentially shifted to an optimum angle for achievement of a specific control target, i.e., MTPA operation or minimum energy consumption over a driving cycle, Fig. 4. Obviously, there is a degree of freedom for the hybrid rotor concept. In the proposed hybrid concept, Fig. 2(a), the two Ferrite rotor stacks are kept aligned to each other. For simplicity, analysis of the hybrid concept via 2D FEA (torque and flux maps as a function of dq -axis currents) is presented. In practice, the axially combined rotor structure with circumferentially shifted angle between the two-rotor parts may result in different dq -axis currents to be seen by the two components. According to Fig. 4, for a given dq -axis currents

(i_d and i_q) applied to the stator winding of the hybrid concept machine, while the applied i_d and i_q currents could still be seen by the Ferrite rotor part, the currents seen by the SynR rotor part in the SynR machine reference, i_{dSynR} and i_{qSynR} , are defined in (1) and (2) where α is the circumferential shifted angle [10].

$$i_{dSynR} = i_d \cos(\alpha) - i_q \sin(\alpha) \quad (1)$$

$$i_{qSynR} = i_d \sin(\alpha) + i_q \cos(\alpha) \quad (2)$$

The results of (1) and (2) could be used to compute the torque and the dq -axis flux linkages of the SynR part in the SynR machine dq -axis reference via predefined 2D FEA torque and flux maps: T_{eSynR} , ψ_{dSynR} , ψ_{qSynR} . Using the obtained values, the torque and the dq -axis flux linkages of the SynR part in the Ferrite machine dq -axis reference, $T_{eSynR(1)}$, $\psi_{dSynR(1)}$, $\psi_{qSynR(1)}$, are expressed in (3) to (5), [10].

$$\psi_{dSynR(1)}(i_d, i_q) = \psi_{dSynR}(i_{dSynR}, i_{qSynR}) \cos(\alpha) + \psi_{qSynR}(i_{dSynR}, i_{qSynR}) \sin(\alpha) \quad (3)$$

$$\psi_{qSynR(1)}(i_d, i_q) = -\psi_{dSynR}(i_{dSynR}, i_{qSynR}) \sin(\alpha) + \psi_{qSynR}(i_{dSynR}, i_{qSynR}) \cos(\alpha) \quad (4)$$

$$T_{eSynR(1)}(i_d, i_q) = T_{eSynR}(i_{dSynR}, i_{qSynR}) \quad (5)$$

Finally, the torque and dq -axis flux linkages of the hybrid concept in the Ferrite machine dq -axis reference, T_{eHyb} , ψ_{dHyb} , ψ_{qHyb} , could be obtained via (6) to (7) where $l_{Ferrite}$ and l_{SynR} is the active length of the Ferrite rotor part and the SynR rotor part, respectively.

$$T_{eHyb}(i_d, i_q) = \frac{l_{Ferrite} T_{eFerrite}(i_d, i_q) + l_{SynR} T_{eSynR(1)}(i_d, i_q)}{l_{Ferrite} + l_{SynR}} \quad (6)$$

$$\psi_{dHyb}(i_d, i_q) = \frac{l_{IPM} \psi_{dFerrite}(i_d, i_q) + l_{SynR} \psi_{dSynR(1)}(i_d, i_q)}{l_{Ferrite} + l_{SynR}} \quad (7)$$

$$\psi_{qHyb}(i_d, i_q) = \frac{l_{IPM} \psi_{qFerrite}(i_d, i_q) + l_{SynR} \psi_{qSynR(1)}(i_d, i_q)}{l_{Ferrite} + l_{SynR}} \quad (8)$$

In the next section, the torque and the dq -axis flux linkages obtained from (6) to (8) is employed to study the optimum shifted angle for the hybrid machine concept.

3 Optimum shifted angle for hybrid machine concept

In Fig. 5, study on circumferential shifted angle to achieve optimum performance for the hybrid concept machine is presented. By varying the shifted angle α in Fig. 4 from 0 to 60 electrical degrees (0 to 12 mechanical degrees), energy loss over WLTP driving cycle [see Figs. 9 and 10] for the hybrid rotor machine concept is depicted in Fig. 5(a) where the energy loss is minimized when the shifted angle is as around 20 electrical degrees. On the other hand, current magnitude with MTPA operation under different shifted angles for the hybrid concept machine compared with the Ferrite machine is presented in Fig. 5(b). As can be seen, for a shifted angle as 20 electrical degrees, in the high torque region, a very similar current magnitude with the Ferrite machine could be obtained.

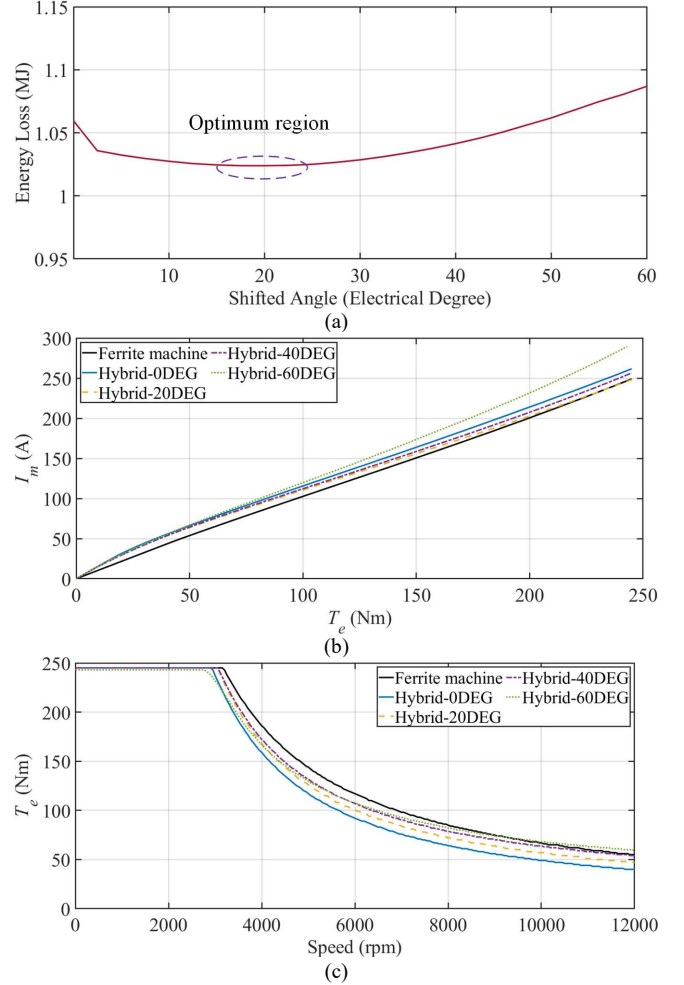


Fig. 5. Hybrid concept performance under different circumferentially shifted angle. (a) Energy loss over WLTP driving cycle. (b) Current magnitude under MTPA operation. (c) Torque-speed envelope.

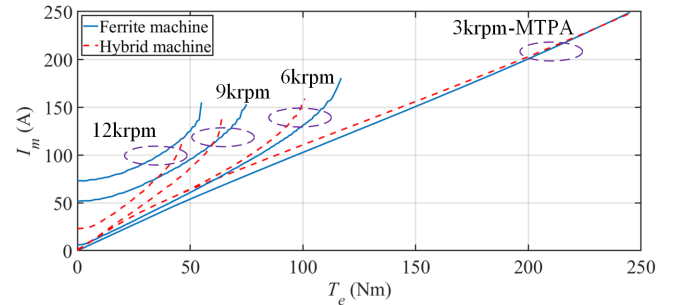


Fig. 6. Current magnitude over demanded torque between hybrid and Ferrite machine under different operation speeds.

In addition, torque-speed envelope of the hybrid concept over different shifted angles compared with the Ferrite benchmark machine is presented in Fig. 5(c) where a lower maximum achievable torque than the Ferrite machine could be observed for the hybrid concept machine in the high-speed region. Also, a shifted angle higher than 20 electrical degrees could result in a higher maximum torque envelop in the high-speed region but with compromising peak torque value in the low-speed region. Fig. 6 presents current magnitudes over demanded torque for the hybrid machine compared with the Ferrite machine. As can be seen, for the hybrid machine in the high-speed low-torque region, significant lower current magnitudes required could be observed.

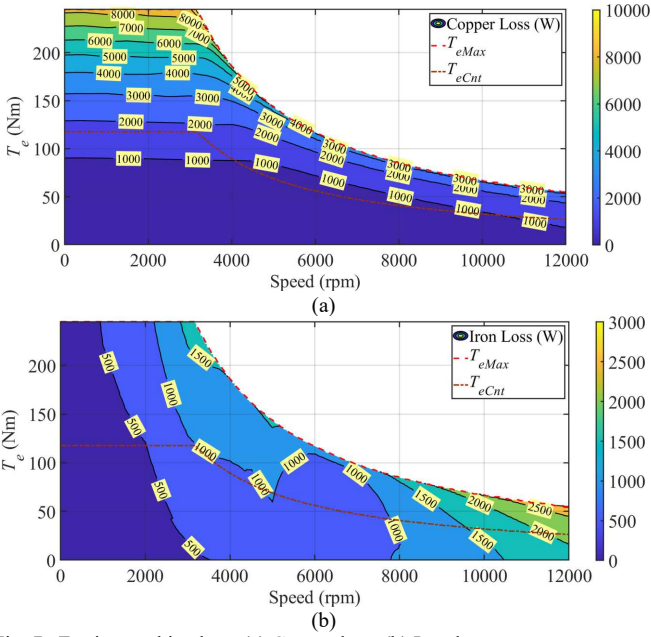


Fig. 7. Ferrite machine loss. (a) Copper loss. (b) Iron loss.

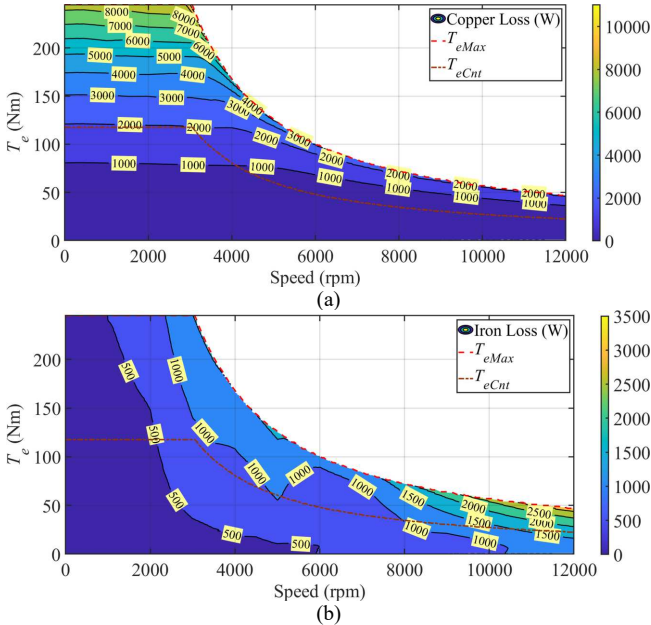


Fig. 8. Hybrid concept machine loss. (a) Copper loss. (b) Iron loss.

4 Performance analysis of hybrid concept

In this section, performance analysis of the hybrid machine focusing on energy consumption is presented with the Ferrite machine acting as the benchmark. In Figs. 7 and 8, loss over torque speed of the Ferrite machine and the hybrid concept machine is respectively illustrated. By comparing between Fig. 7(a) and 8(a), in the low-torque/low-speed region, copper loss under the hybrid concept is higher than the Ferrite machine. However, in the high-torque/low-speed region, a very similar copper losses compared with the Ferrite machine could be achieved for the hybrid machine. In addition, in the low-torque/high-speed region, significant lower copper losses could be observed for the hybrid machine. Obviously, the copper loss in Figs. 7(a) and 8(a) is in good arrangement with the current magnitude over demanded torque in Fig. 6.

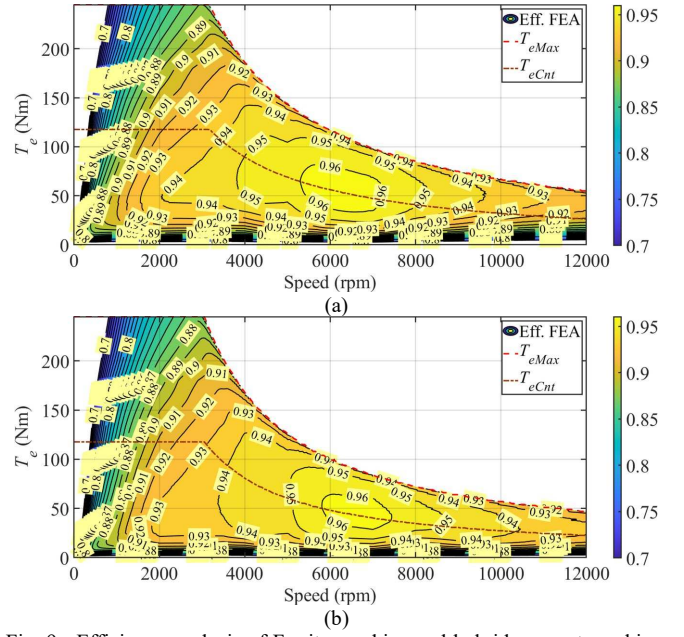


Fig. 9. Efficiency analysis of Ferrite machine and hybrid concept machine. (a) Ferrite machine. (b) Hybrid concept machine.

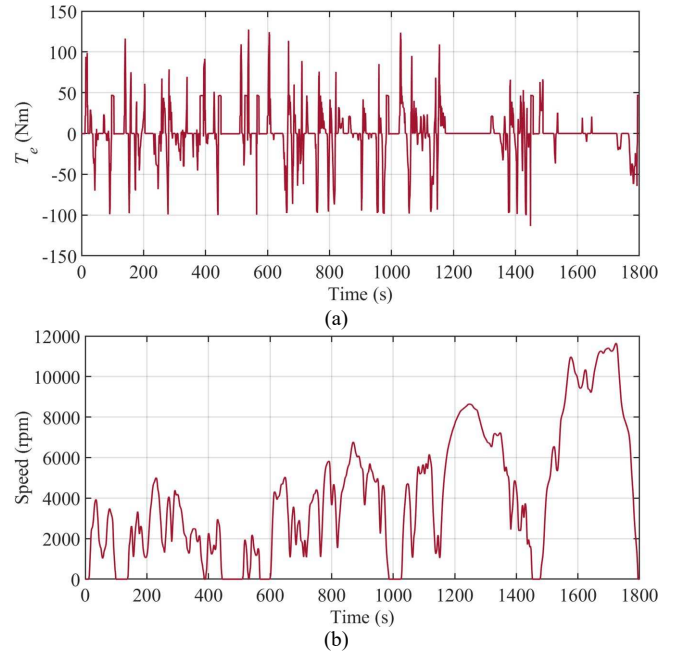


Fig. 10. WLTP driving cycle for energy consumption evaluation. (a) Traction machine torque. (b) Traction machine speed.

On the other hand, significant lower iron losses over torque speed performance for the hybrid machine could be seen in Fig. 8(b) compared with that of the Ferrite machine shown in Fig. 7(b).

To further demonstrate the hybrid concept, efficiency over torque-speed performance of the hybrid machine is depicted in Fig. 9(b) and the relevant efficiency for the Ferrite machine is presented in Fig. 9(a). As can be seen, a maximum efficiency up to 97% could be achieved for the hybrid concept which is comparable with that of the Ferrite machine shown in Fig. 9(a). In addition, due to the lower losses for the hybrid concept in the high-speed region [see Figs. 7 and 8], up to 1% higher in efficiency could be observed for the hybrid concept, Fig. 9(b).

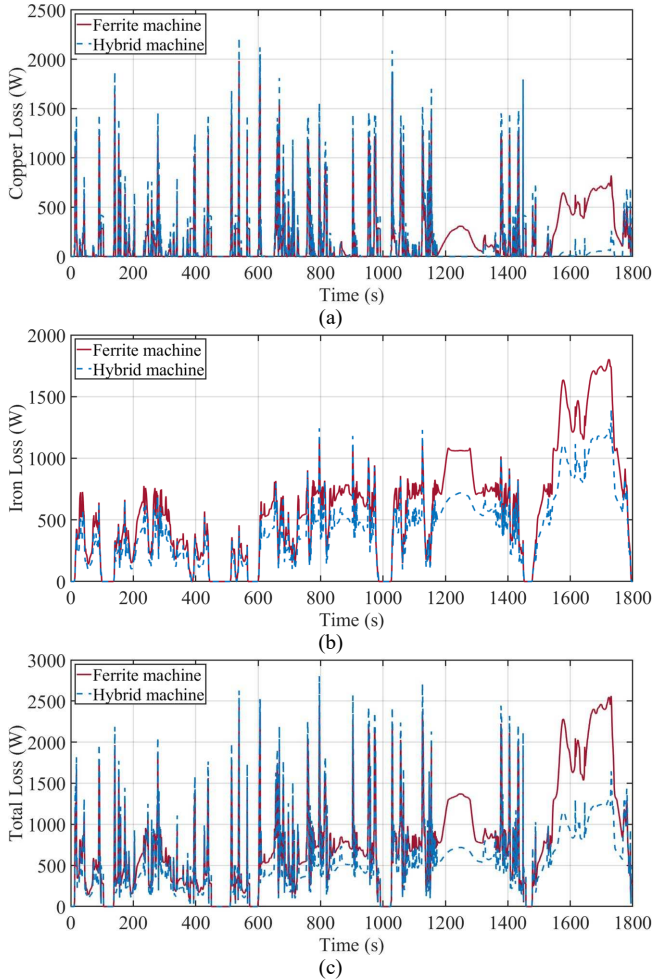


Fig. 11. Losses over WLTP driving cycle for Ferrite machine and hybrid concept machine. (a) Copper loss. (b) Iron loss. (c) Total loss.

In Fig. 10, the WLTP driving cycle for energy consumption evaluation of the hybrid concept machine is depicted and the relevant losses of the Ferrite and hybrid concept machines are presented in Fig. 11. As can be seen, in the high-speed region, due to the lower d -axis current required for maintaining the maximum voltage magnitude, lower copper losses could be observed for the hybrid machine in Fig. 11(a). In addition, Fig. 11(b) shows that a lower iron loss could also be achieved. The advantage in terms of total losses for the hybrid concept machine over the Ferrite machine is highly demonstrated in Fig. 11(c).

Based on Fig. 11, the differences in energy loss over the WLTP driving cycle between the hybrid concept machine and the Ferrite benchmark machine is presented in Table 2. As can be seen, up to 26.29% reduction of the total energy consumption could be achieved for the hybrid concept machine. Also, a reduction up to 22.29% in copper energy loss and 27.64% in iron energy loss could be respectively obtained for the hybrid concept.

Table 2 Energy loss over WLTP driving cycle (MJ)

Component	Ferrite	Hybrid	Diff. %
Copper Loss	0.3369	0.2618	-22.29
Iron Loss	1.053	0.762	-27.64
Total Loss	1.389	1.0239	-26.29

5 Conclusion

The paper presents performance analysis of a hybrid Ferrite Interior Permanent Magnet (IPM)/synchronous reluctance (SynR) traction machine with axially combined rotor structure. First, a hybrid rotor with axially combined structure of Ferrite IPM-rotor part and SynR rotor-part is introduced. Then, performance analysis of the machine is presented. It is shown that due to the axially combined structure, the hybrid machine concept could achieve a significant lower copper and iron loss, especially in the high-speed operation region, compared with the original Ferrite IPM machine. It is demonstrated that due to the difference in optimum operation between the IPM and SynR machines, the two-rotor parts could be circumferentially shifted by an optimum angle for a specific control target achievement, i.e., maximum torque per ampere (MTPA) or minimum energy consumption over a specific driving cycle. Therefore, an extra degree of freedom could be obtained. The proposed concept is validated via FEA benchmarking by a high-speed high-power (12,000rpm and 80kW) Ferrite IPM traction machine. It is presented that in comparison with the Ferrite IPM benchmark machine, a reduction up to 26.29% in energy consumption over WLTP driving cycle could be achieved for the proposed hybrid rotor machine.

6 References

- [1] K. D. Hoang, P. Lazari, K. Atallah, J. G. Birchall and S. D. Calverley, "Evaluation of simplified model for rapid identification and control development of IPM traction machines," in *IEEE Transactions on Transportation Electrification*, vol. 7, no. 2, pp. 779-792, June 2021.
- [2] K. D. Hoang, "Simplified analytical model for rapid evaluation of interior PM traction machines considering magnetic nonlinearity," in *IEEE Open Journal of the Industrial Electronics Society*, vol. 1, pp. 340-354, 2020.
- [3] K. Atallah and J. Wang, "A rotor with axially and circumferentially magnetized permanent magnets," in *IEEE Trans. Magnetics*, vol. 48, no. 11, pp. 3230-3233, Nov. 2012.
- [4] A. Shanshal, K. Hoang and K. Atallah, "High-performance Ferrite permanent magnet brushless machines," in *IEEE Transactions on Magnetics*, vol. 55, no. 7, pp. 1-4, July 2019.
- [5] M. Ferrari, N. Bianchi, A. Doria and E. Fornasiero, "Design of synchronous reluctance motor for hybrid electric vehicles," in *IEEE Transactions on Industry Applications*, vol. 51, no. 4, pp. 3030-3040, July-Aug. 2015.
- [6] B. J. Chalmers, R. Akmes, and L. Musaba, "Design and field-weakening performance of permanent-magnet/reluctance motor with two-part rotor," *Proc. Inst. Elect. Eng.*, pt. B, vol. 145, no. 2, pp. 133-139, 1998.
- [7] N. Bianchi, S. Bolognani and B. J. Chalmers, "Salient-rotor PM synchronous motors for an extended flux-weakening operation range," in *IEEE Transactions on Industry Applications*, vol. 36, no. 4, pp. 1118-1125, July-Aug. 2000.
- [8] W. Zhao, H. Shen, T. A. Lipo and X. Wang, "A new hybrid permanent magnet synchronous reluctance machine with axially sandwiched magnets for performance improvement," in *IEEE Transactions on Energy Conversion*, vol. 33, no. 4, pp. 2018-2029, Dec. 2018.
- [9] J. -X. Shen, Y. -Q. Lin, Y. Sun, X. -F. Qin, W. -J. Wan and S. Cai, "Permanent magnet synchronous reluctance machines with axially combined rotor structure," in *IEEE Transactions on Magnetics*, vol. 58, no. 2, pp. 1-10, Feb. 2022.
- [10] K. D. Hoang, P. Lazari and K. Atallah, "Analysis and control development of IPM traction machines with skewed rotor using unskewed machine model," *IECON 2021 - 47th Annual Conference of the IEEE Industrial Electronics Society*, 2021, pp. 1-6.